Supporting information for

Size-induced amorphous structure in tungsten oxide nanoparticles

*Mikkel Juelsholt,[1] Andy S. Anker,[1] Troels Lindahl Christiansen,[1] Mads Ry Jørgensen,[2,3] Innokenty Kantor,[2,4] Daniel Risskov Sørensen,[2,3] and Kirsten M. Ø Jensen[1]**

1: Department of Chemistry and Nano-Science Center, University of Copenhagen, 2100 Copenhagen Ø, Denmark

2: Department of Chemistry & iNANO, Aarhus University, 8000 Aarhus C, Denmark

3: MAX IV Laboratory, Lund University, 224 84 Lund

4: Department of Physics, The Technical University of Denmark, 2880 Lyngby, Denmark

Table of Contents:

A: Extended range of PDFs obtained from the crystalline nanoparticles

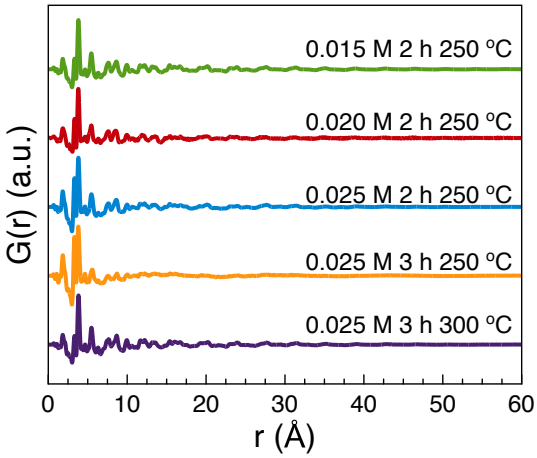

Figure S1: Pair distribution functions (PDFs) obtained from the nanorods plotted to 60 Å.

B: Small-Angle X-ray Scattering

Aggregation of the nanoparticles

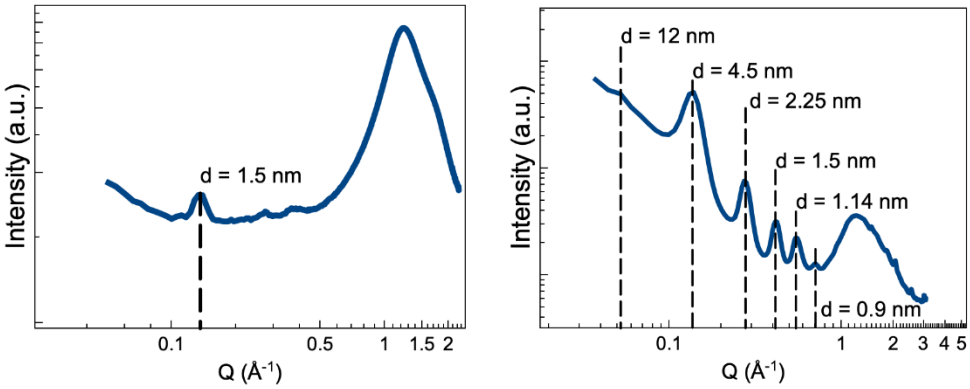

Figure S2: Left: SAXS pattern for the 10 mM sample in a toluene suspension. The sample had been left undisturbed for 48 h before measurements. Right: SAXS pattern for the 5 mM sample in a toluene suspension. The sample has been left undisturbed for 12 h before measurements. In both cases, this led to the formation of a nanostructured lattice. The arrows indicate the main peaks arising from the ordered nanoparticle lattice and the corresponding d-spacing. The large broad peak at 1.22 $Å^{-1}$ arises from toluene. The SAXS data are plotted on a double logarithmic scale.

The SAXS pattern from WO_x samples left undisturbed for 12-48 hours clearly shows several diffraction peaks where the main ones are indicated in Figure S2 together with their corresponding d-spacings. The d-spacing of 4.5 nm seen for the 5 mM samples agrees with the diameter of a nanoparticle (2 nm) and one ligand, oleylamine (2 nm in length). As shown in Figure 3A in the main text, the nanoparticles in this sample are ca. 2 nm in diameter and oleylamine is also around 2 nm long.[1] We have not been able to relate the other d-spacings observed in the SAXS pattern to a specific nanoparticle lattice, and they may also relate to oleylamine interactions.

SAXS Data Modelling

When using fast sample preparation and limited measurement time, it was possible to gain SAXS data with limited particle-particle interaction which could be modelled with a simple model. The SAXS patterns in the main text were obtained by taking 2 mL of the unwashed nanoparticle suspension into 20 mL of toluene and then ultrasonicate the suspension for approximately 2 hours. The solution was then transferred to a borosilicate capillary. The sealed capillary was loaded into the instrument and data were measured for 2 h. The SAXS pattern from toluene in a borosilicate capillary was used as background.

The size and shape of the nanoparticles formed at 5 and 10 mM could be modelled using a spherical form factor and a log-normal size distribution as implemented in Diffpy-CMI,[2] using SASView functions.[3] The particle-particle interactions were described with a combination of two models. At high Q-values which correspond to short distances, the interactions could be modelled using a hard-sphere structure factor as implemented in SASview.[3-5] This model took two parameters, a volume fraction which describes how strong the particle-particle interaction is, and an effective radius which is the distance between the center of two interacting particles. In the best models the effective radius refined to 4 nm. For the smallest nanoparticles synthesized at 5 mM this corresponds to twice the radius (1 nm) of two nanoparticles, around 2 nm, and 1 oleylamine ligand, also around 2 nm. For the nanoparticles synthesized at 10 mM an effective radius of 4 nm only corresponds to two times the radius of the nanoparticles, which suggests that the nanoparticles synthesized at 10 mM interact much more directly with each other.

At low Q-values, corresponding to large distances, the SAXS data took the form of a straight line when plotted at a log-log scale. This indicates particle aggregation in the sample,[6,7] which

is to be expected when there are particle-particle interactions. The scattering from the aggregate is commonly described using a power law, Q^{-D}, where the value of D can be interpreted as the dimensionality of the aggregation.[6,7] In our case the 5 mM sample was best described using D = 1 and the 10 mM sample was best described using D = 3.

Table S1: Refined parameters for the fit seen in Figure 3A

	5 mM	
Volume fraction	**Effective radius**	**D**
0.045	39.8 Å	1
Radius	**Dispersity**	**Background**
9.38 Å	0.52	0.0023

Table S2: Refined parameters for the fit seen in Figure 3B

	10 mM	
Volume fraction	**Effective radius**	**D**
0.25	40.1 Å	3
Radius	**Dispersity**	**Background**
23 Å	0.51	0.00038

C: Pair Distribution Function analysis of amorphous nanoparticles

For modeling of the PDFs from amorphous samples, starting models were obtained from reported crystal structures of metatungstate and paratungstate. The metatungstate cluster was obtained from the crystal structure reported by Niu et al.[8] and the paratungstate cluster was obtained from the crystal structure reported by Averbuch-Pouchot et al.[9] The clusters were manually carved out of the crystal. This was done by expanding the crystal structure into a 2x2x2 supercell in Vesta[10] and removing atoms until only one cluster remained. This cluster was then saved as a xyx-file. To produce the paratungstate cluster fragments the paratungstate cluster was loaded into Vesta and octahedra were removed manually one at a time. The obtained paratungstate fragments were also saved as xyz-files and fitted to the experimental PDF using Diffpy-CMI.[2]

These structures were modelled as discrete structures to the PDF, i.e. without the assumption of periodic order. Here, the scale factor, was refined along with atomic displacement parameters (ADPs) for the atoms in the structure. The ADPs were constrained so that one, isotropic ADP was used for all W atoms, and one isotropic ADP was used for all O atoms. The atomic positions of the W atoms were also refined, but the W atoms were only allowed to move up to 0.05 Å.

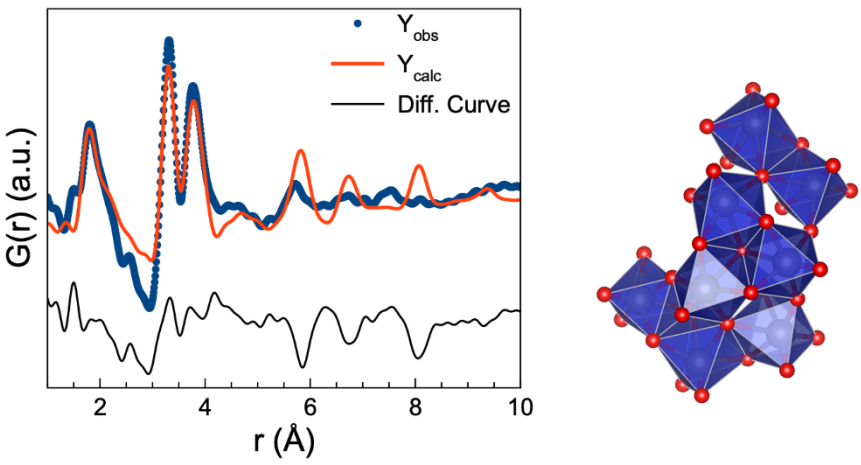

Figure S3: Fit of a paratungstate fragment containing 8 [WO_6]-octahedra to the PDF obtained from the 5 mM sample. The resulting structure is seen on the right.

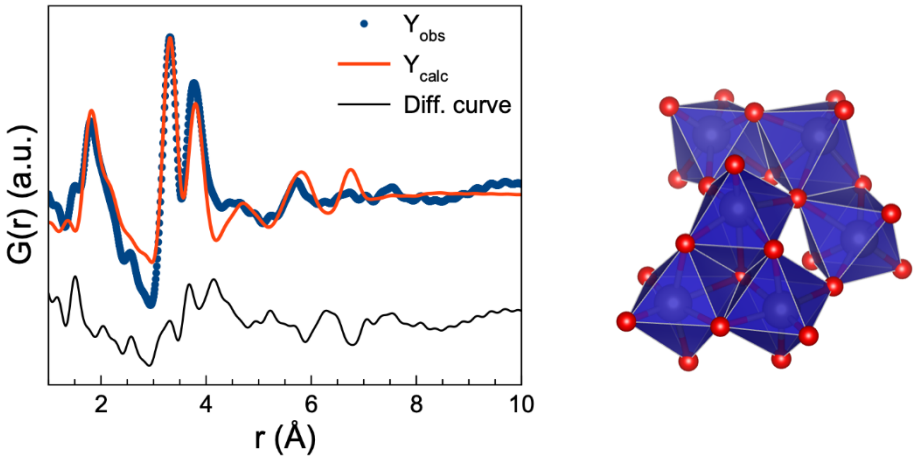

Figure S4: Fit of a paratungstate fragment containing 6 [WO_6]-octahedra to the PDF obtained from the 5 mM sample. The resulting structure is seen on the right.

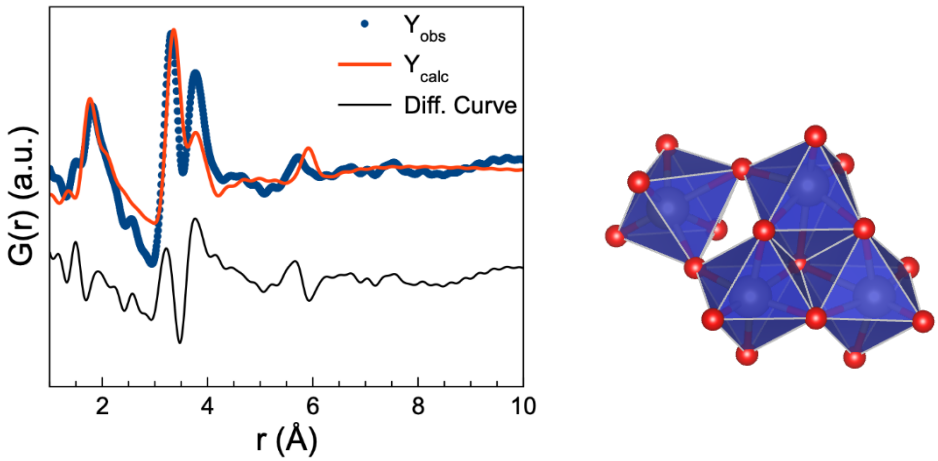

Figure S5: Fit of a paratungstate fragment containing 4 [WO_6]-octahedra to the PDF obtained from the 5 mM sample. The resulting structure is seen on the right.

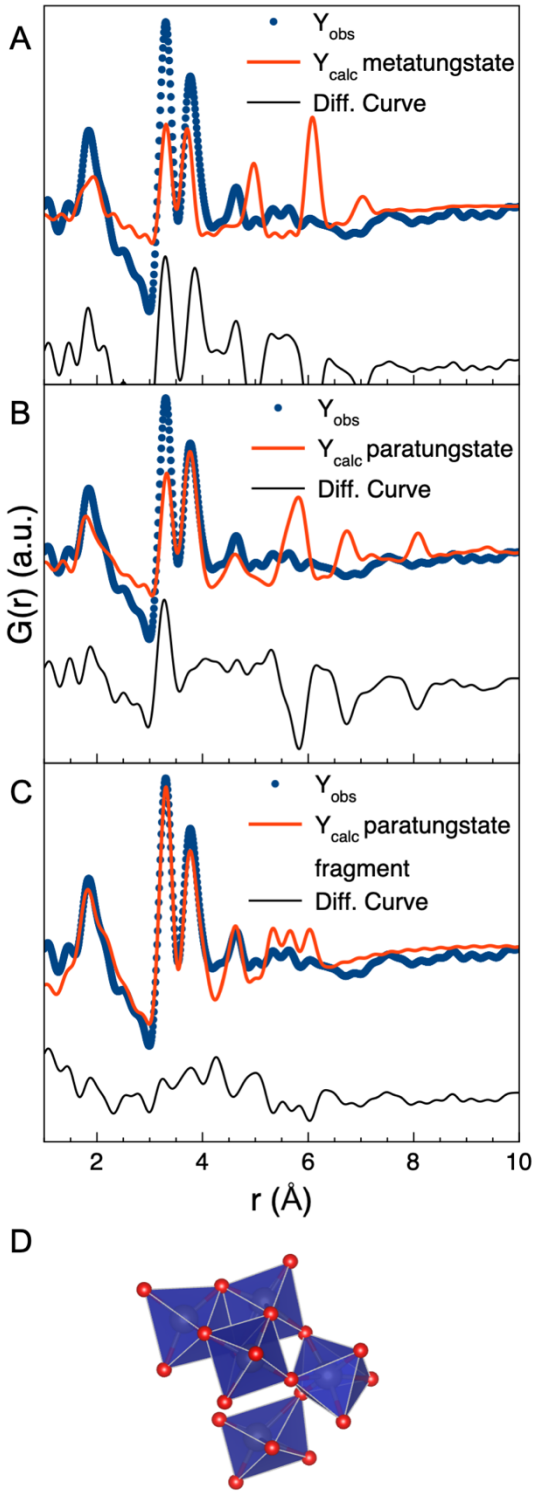

Figure S6: (A) The fit of metatungstate to the PDF obtained from the 10 mM sample. (B) The fit of paratungstate. (C) The fit of the structure seen in (D).

D: TEM Images

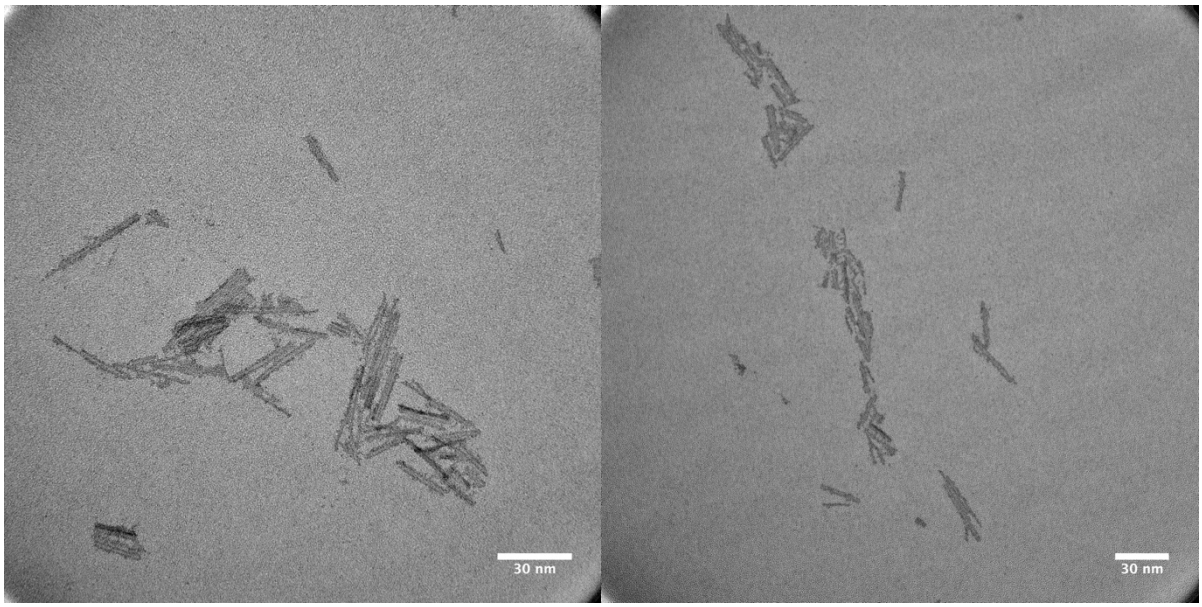

Figure S7: Two TEM images of the nanoparticles formed at 15 mM at 250 ºC.

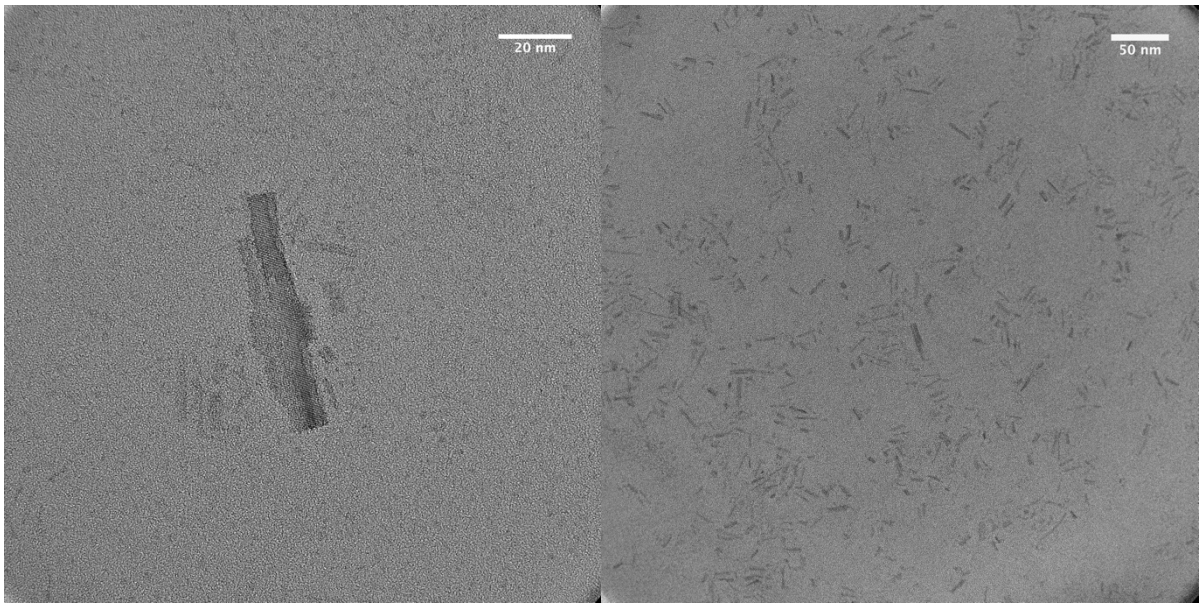

Figure S8: Two TEM images of the nanoparticles formed at 20 mM at 250 ºC.

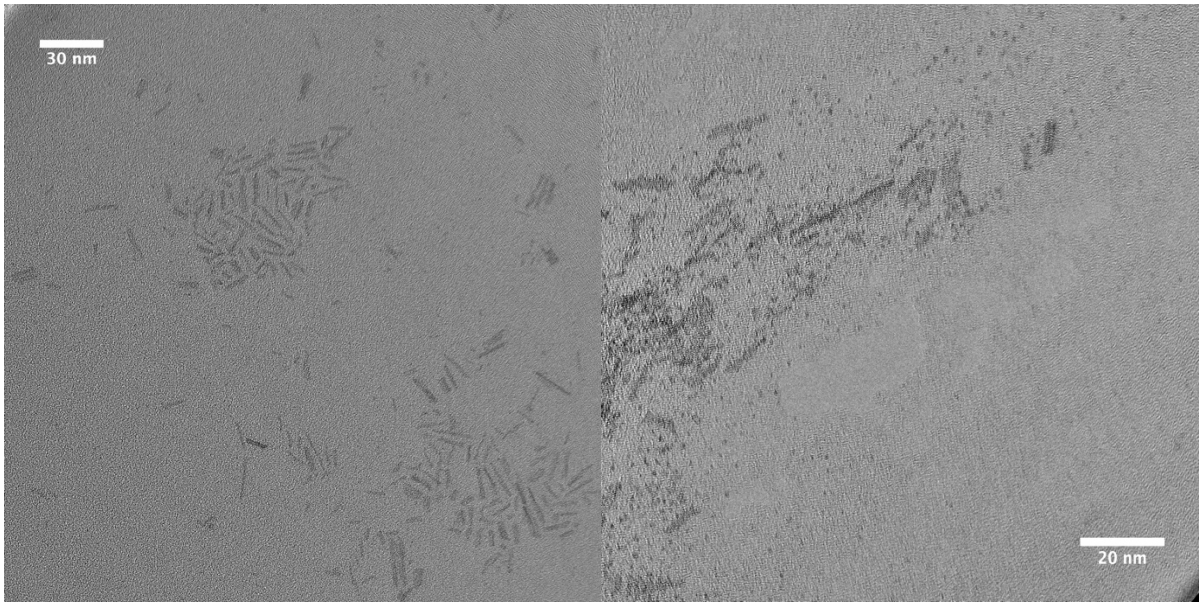

Figure S9: Two TEM images of the nanoparticles formed at 25 mM at 250 ºC.

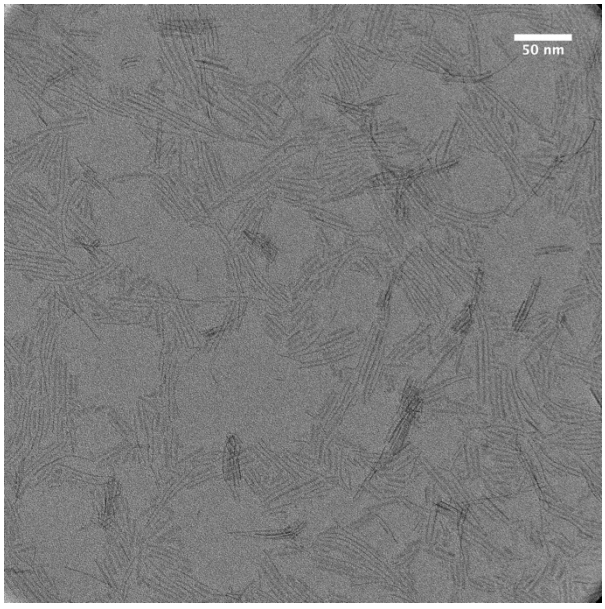

Figure S10: A TEM image of the nanoparticles formed at 25 mM at 300 ºC.

E: PDF analysis of the crystalline nanoparticles

The PDF obtained from the 15 mM sample was modelled using PDFgui,[11] while all other PDFs were treated using Diffpy-CMI.[2] In both cases, starting models for the crystalline materials were obtained from the Inorganic Crystal Structure Database (ICSD) or the Crystallography Open Database (COD).[12-14] Only crystal structures that included the O atomic positions were considered. Based on the models, a PDF was calculated, and the relevant structural parameters were fitted to the experimental PDF. The scale factor, lattice parameters, δ_2, atomic positions, isotropic Atomic Displacement Parameters and a spherical particle diameter were refined for the crystalline phases. All models were modified such that all metal positions were fully occupied by W.

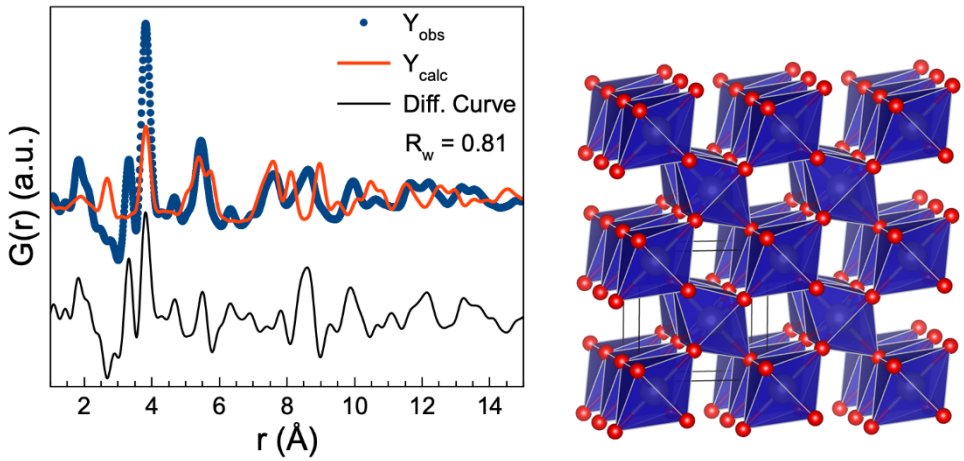

Figure S11: Fit to the PDF obtained from the nanoparticles synthesized at 15 mM at 250 °C using WO_2. The crystal structure is seen to the right.

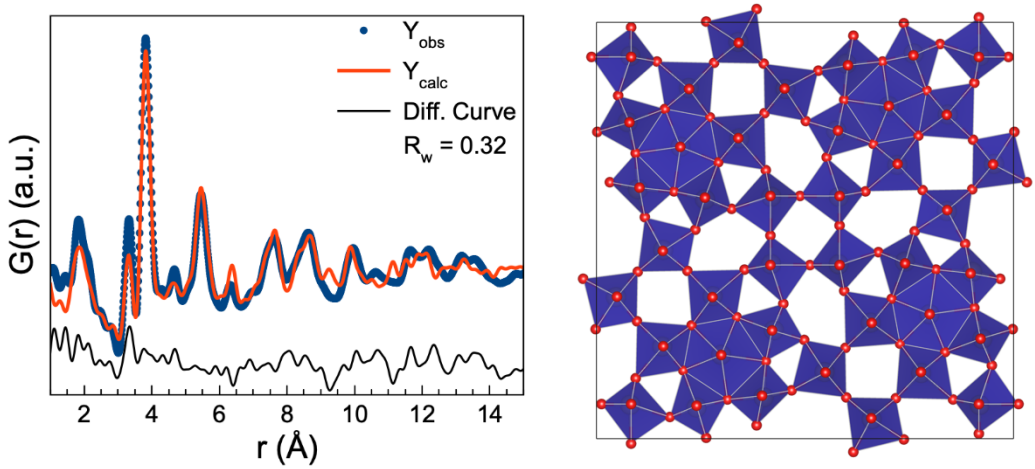

Figure S12: Fit to the PDF obtained from the nanoparticles synthesized at 15 mM at 250 °C using W_5O_{14}. The crystal structure is seen to the right.

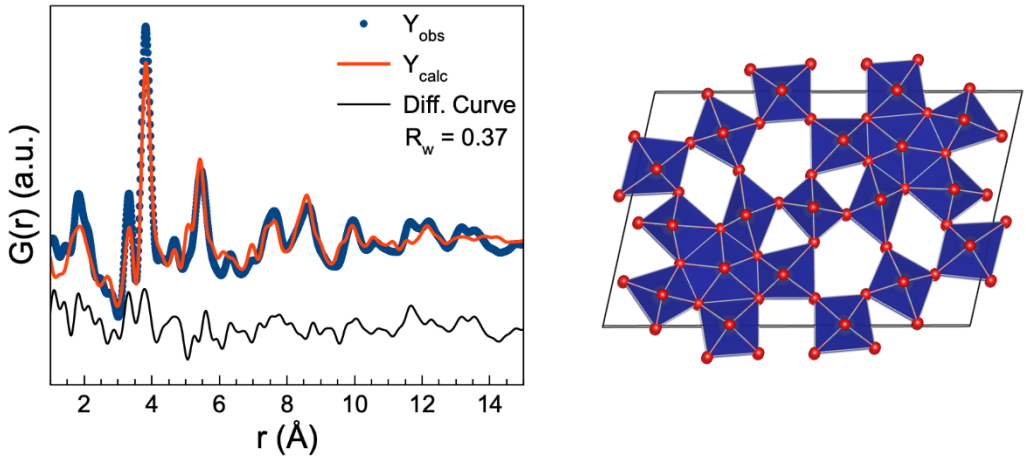

Figure S13: Fit to the PDF obtained from the nanoparticles synthesized at 15 mM at 250 °C using $W_{17}O_{47}$. The crystal structure is seen to the right.

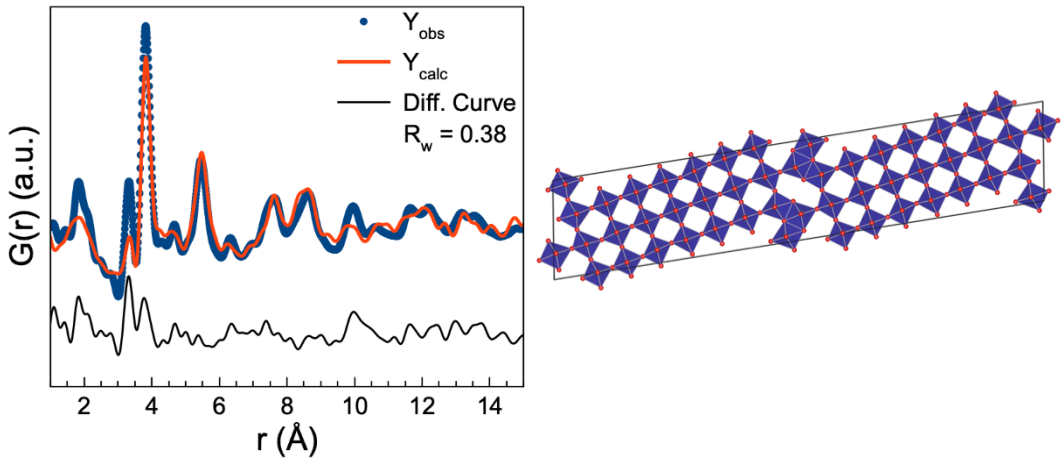

Figure S14: Fit to the PDF obtained from the nanoparticles synthesized at 15 mM at 250 °C using $W_{25}O_{73}$. The crystal structure is seen to the right.

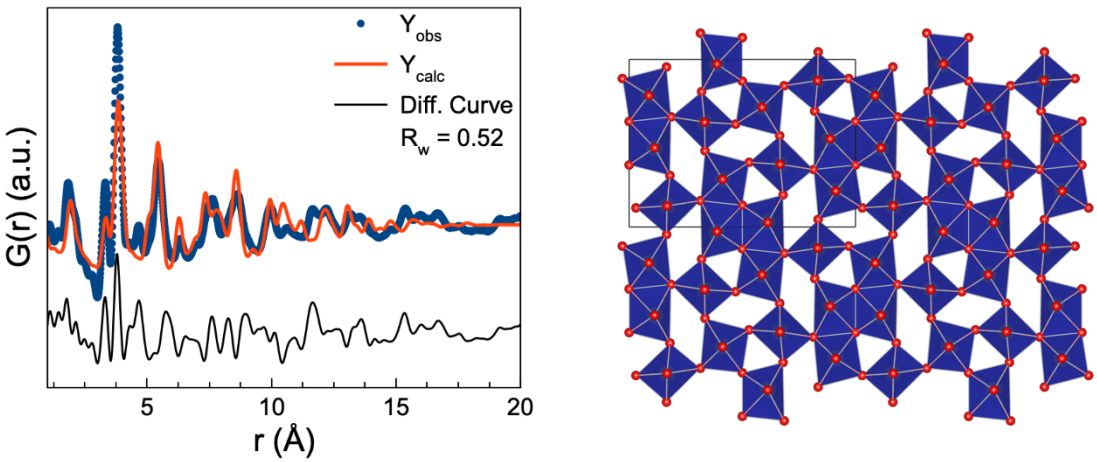

Figure S15: Fit to the PDF obtained from the nanoparticles synthesized at 15 mM at 250 °C using one of two previously reported W_3O_8 phases. The crystal structure is seen to the right.

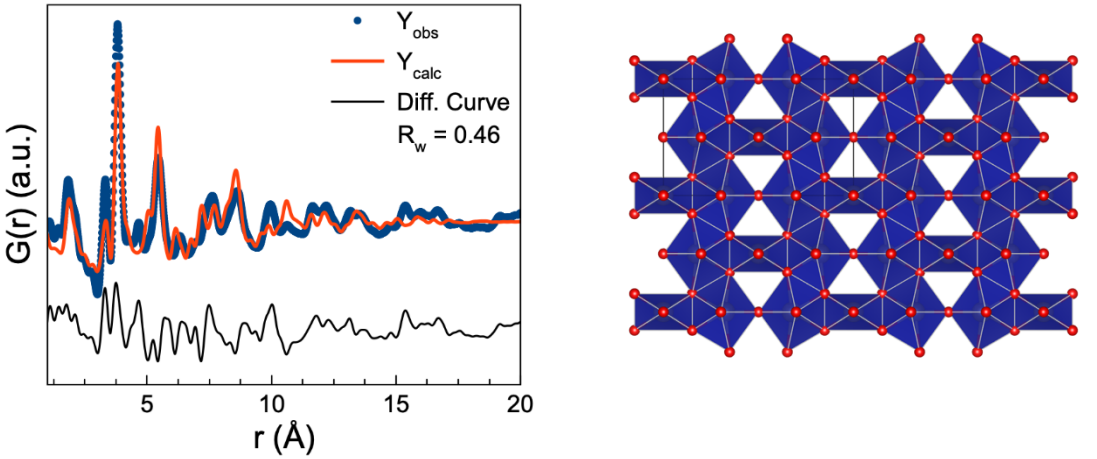

Figure S16: Fit to the PDF obtained from the nanoparticles synthesized at 15 mM at 250 °C using the second of the two previously reported W_3O_8 phases. The crystal structure is seen to the right.

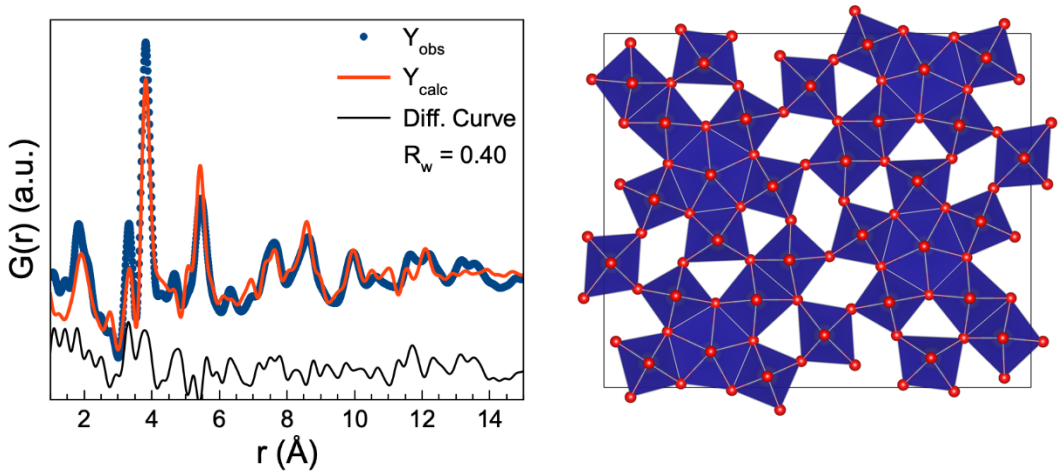

Figure S17: Fit to the PDF obtained from the nanoparticles synthesized at 15 mM at 250 ºC using $W_{32}O_{84}$. The crystal structure is seen to the right.

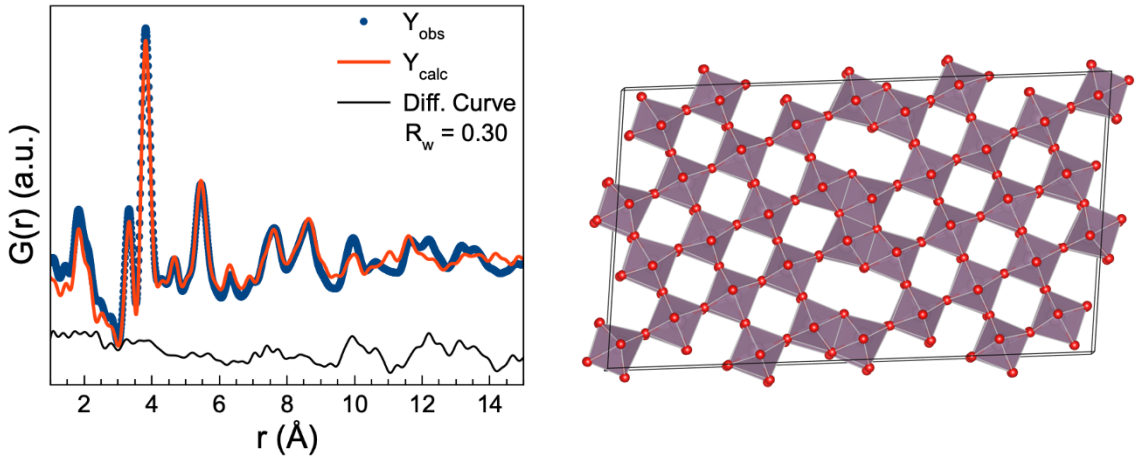

Figure S18: Fit to the PDF obtained from the nanoparticles synthesized at 15 mM at 250 ºC using Mo_9O_{26}. The crystal structure is seen to the right.

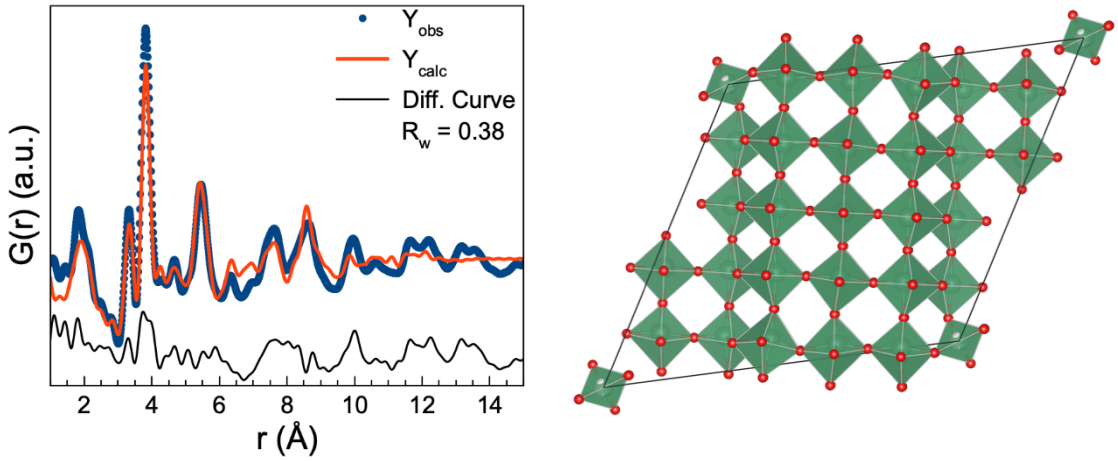

Figure S19: Fit to the PDF obtained from the nanoparticles synthesized at 15 mM at 250 °C using H-Nb_2O_5. The crystal structure is seen to the right.

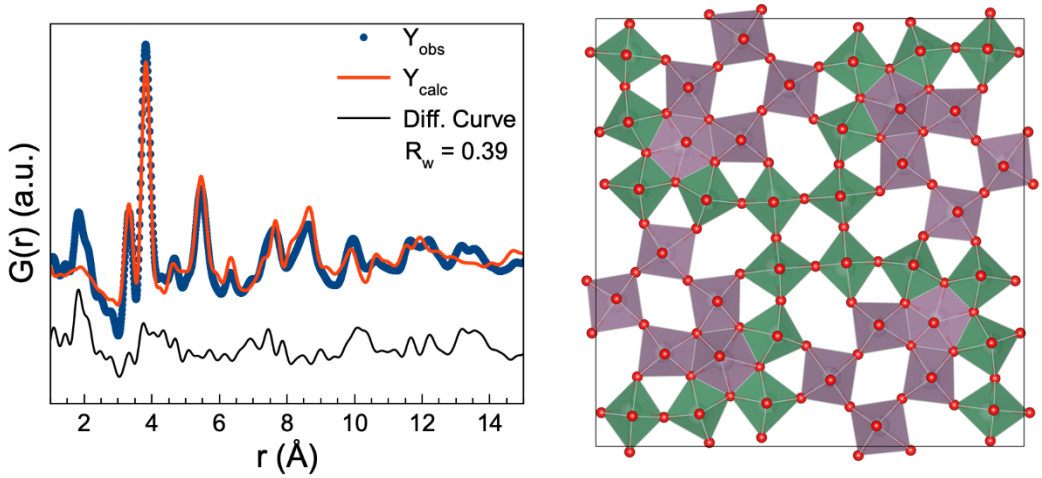

Figure S20: Fit to the PDF obtained from the nanoparticles synthesized at 15 mM at 250 °C using $Nb_2Mo_3O_{14}$. The crystal structure is seen to the right. The colors of the polyhedra do not reflect the occupancies of the individual sites, but merely show that this structure contains both Nb and Mo.

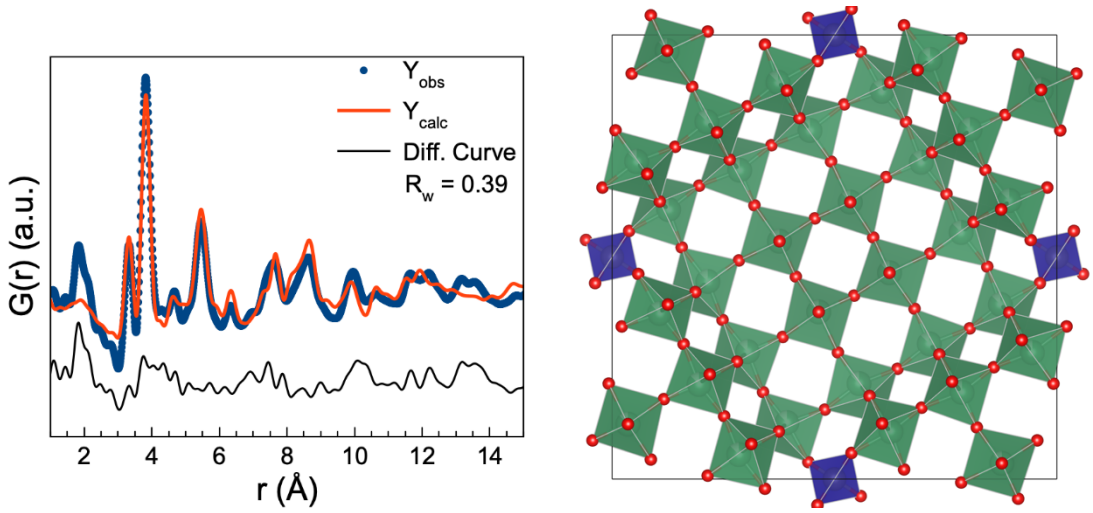

Figure S21: Fit to the PDF obtained from the nanoparticles synthesized at 15 mM at 250 °C using $Nb_{14}W_3O_{44}$. The crystal structure is seen to the right. The colors of the polyhedra do not reflect the occupancies of the individual sites, but merely show that this structure contains both Nb and W.

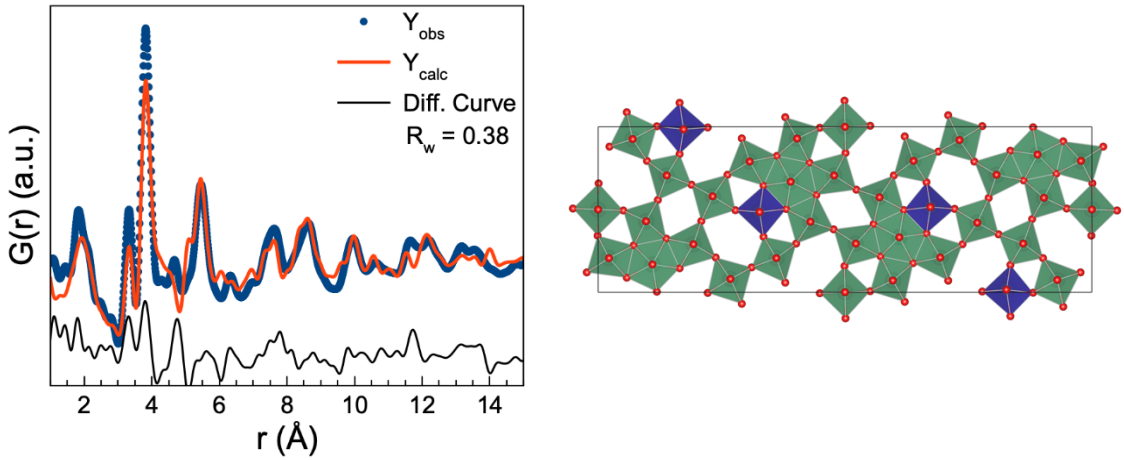

Figure S22: Fit to the PDF obtained from the nanoparticles synthesized at 15 mM at 250 °C using $Nb_{16}W_{18}O_{94}$. The crystal structure is seen to the right. The colors of the polyhedra do not reflect the occupancies of the individual sites, but merely show that this structure contains both Nb and W.

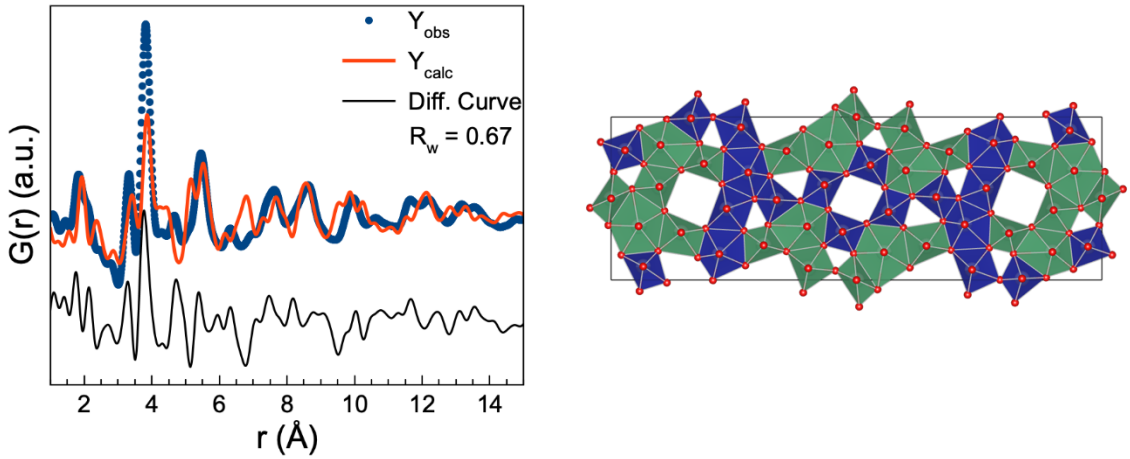

Figure S23: Fit to the PDF obtained from the nanoparticles synthesized at 15 mM at 250 °C using $Nb_{22}W_{20}O_{102}$. The crystal structure is seen to the right. The colors of the polyhedra do not reflect the occupancies of the individual sites, but merely show that this structure contains both Nb and W.

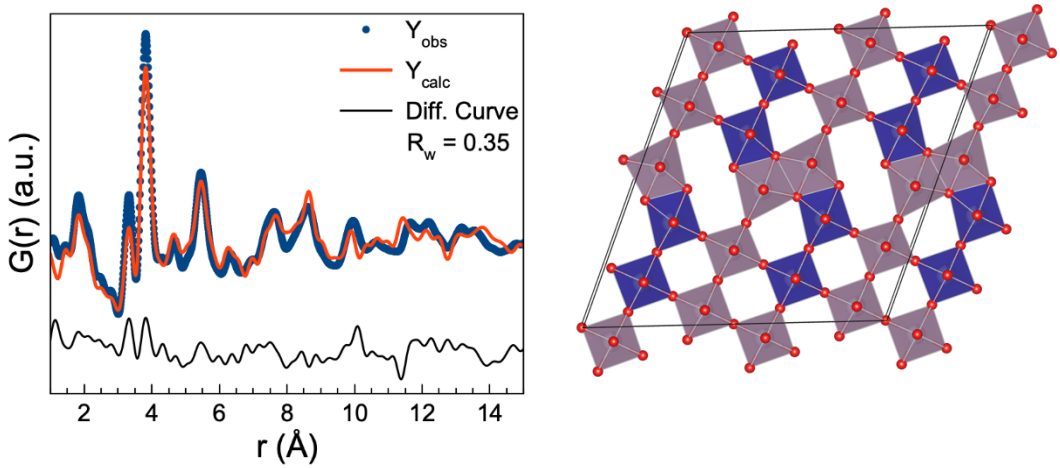

Figure S24: Fit to the PDF obtained from the nanoparticles synthesized at 15 mM at 250 °C using $Mo_5W_5O_{29}$. The crystal structure is seen to the right. The colors of the polyhedra do not reflect the occupancies of the individual sites, but merely show that this structure contains both W and Mo.

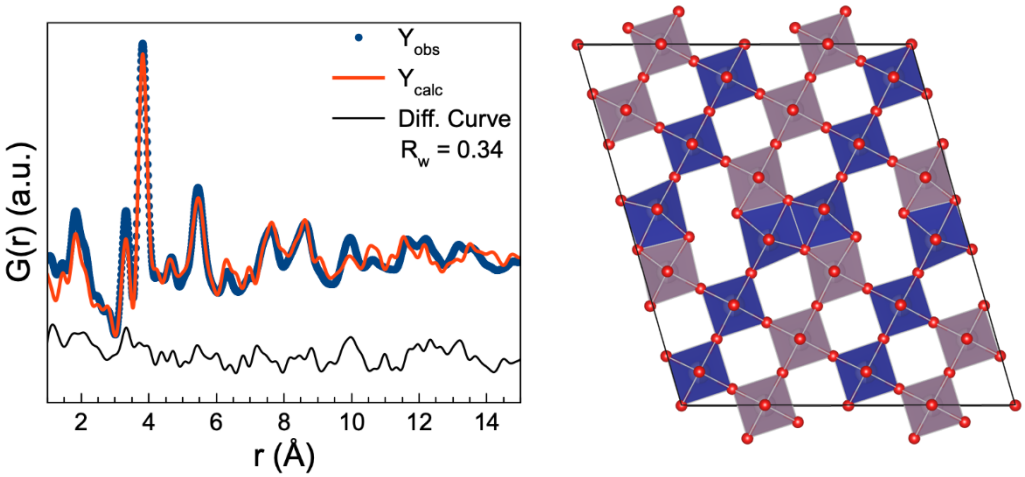

Figure S25: Fit to the PDF obtained from the nanoparticles synthesized at 15 mM at 250 °C using $Mo_{5.5}W_{5.5}O_{32}$. The crystal structure is seen to the right. The colors of the polyhedra do not reflect the occupancies of the individual sites, but merely show that this structure contains both W and Mo.

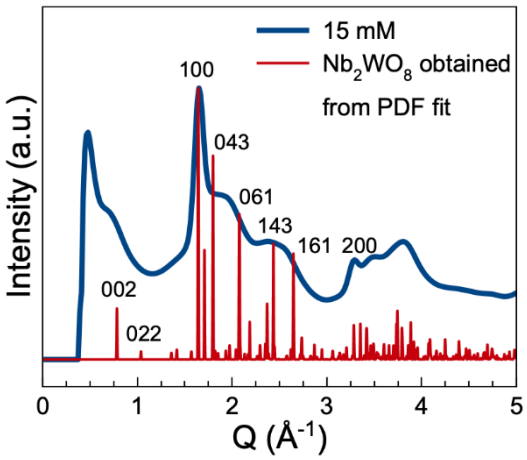

Figure S26: The scattering pattern measured from the nanoparticles synthesized at 15 mM 250 °C compared to the calculated diffraction pattern from the structure obtained from the PDF fit seen in Figure 6C in the main text.

Combined PDF refinements of crystalline models and the amorphous cluster model

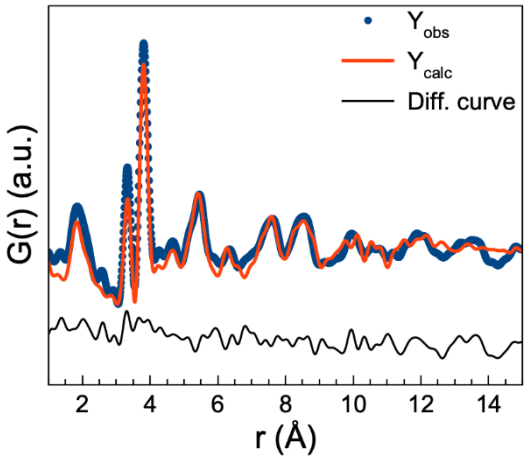

Figure S27: The fit of only the W-substituted Nb_2WO_8 structure to the PDF obtained from the 20 mM sample.

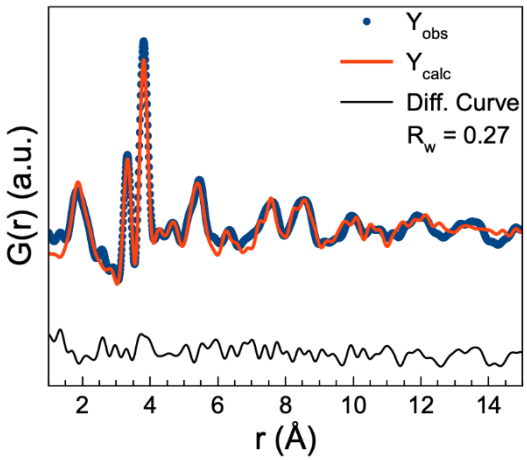

Figure S28: The fit of the W-substituted Nb_2WO_8 structure and the model amorphous structure to the PDF obtained from the 20 mM sample. Refined parameters are seen in Table S8.

Tables of refined parameters for the crystalline models

Table S3: Refined parameters for the fit seen in Figure 6A in the main text.

	$W_{18}O_{49}$	Space group	$P2_1/m$		
	a	**b**	**c**	β	
	19.06 Å	3.84 Å	13.82 Å	115.55°	
	x	**y**	**z**	**U_{iso} (Å^2)**	**occ**
W1	0.920	0.5	0.011	0.004	1
W2	0.941	0.5	0.734	0.004	1
W3	0.860	0.5	0.263	0.004	1
W4	0.771	0.5	0.466	0.004	1
W5	0.736	0.5	0.965	0.004	1
W6	0.713	0.5	0.753	0.004	1
W7	0.648	0.5	0.176	0.004	1
W8	0.568	0.5	0.457	0.004	1
W9	0.536	0.5	0.865	0.004	1
O1	0.923	0.0	0.996	0.05	1
O2	0.919	0.0	0.723	0.05	1
O3	0.87	0.0	0.232	0.05	1
O4	0.78	0.0	0.421	0.05	1
O5	0.744	0.0	0.989	0.05	1
O6	0.724	0.0	0.754	0.05	1
O7	0.638	0.0	0.125	0.05	1
O8	0.587	0.0	0.462	0.05	1
O9	0.551	0.0	0.835	0.05	1
O10	0.983	0.5	0.289	0.05	1
O11	0.964	0.5	0.879	0.05	1
O12	0.864	0.5	0.09	0.05	1
O13	0.857	0.5	0.569	0.05	1
O14	0.853	0.5	0.359	0.05	1
O15	0.805	0.5	0.903	0.05	1
O16	0.812	0.5	0.722	0.05	1
O17	0.757	0.5	0.141	0.05	1
O18	0.694	0.5	0.275	0.05	1
O19	0.689	0.5	0.456	0.05	1
O20	0.66	0.5	0.835	0.05	1
O21	0.649	0.5	0.615	0.05	1
O22	0.629	0.5	0.984	0.05	1
O23	0.535	0.5	0.121	0.05	1
O24	0.486	0.5	0.69	0.05	1
O25	0.5	0.5	0.5	0.05	1
	R_w	**Scale factor**	**SP diameter**	**δ_2**	
	0.38 %	1.215	18.86 Å	3.07 Å^2	

Table S4: Refined parameters for the fit seen in Figure 6B in the main text.

	$W_{10}O_{29}$	Space group	$P2_1/m$		
	a	**b**	**c**	b	
	12.06 Å	3.83 Å	22.31 Å	90.38°	
	x	**y**	**z**	**U_{iso} (Å^2)**	**occ**
W1	0.647	0.5	0.974	0.009	1
W2	0.937	0.5	0.923	0.009	1
W3	0.227	0.5	0.872	0.009	1
W4	0.519	0.5	0.822	0.009	1
W5	0.808	0.5	0.771	0.009	1
W6	0.097	0.5	0.72	0.009	1
W7	0.39	0.5	0.669	0.009	1
W8	0.678	0.5	0.618	0.009	1
W9	0.97	0.5	0.568	0.009	1
W10	0.26	0.5	0.517	0.05	1
O1	0.647	0.0	0.974	0.05	1
O2	0.937	0.0	0.923	0.05	1
O3	0.227	0.0	0.872	0.05	1
O4	0.519	0.0	0.822	0.05	1
O5	0.808	0.0	0.771	0.05	1
O6	0.097	0.0	0.72	0.05	1
O7	0.39	0.0	0.669	0.05	1
O8	0.678	0.0	0.618	0.05	1
O9	0.97	0.0	0.568	0.05	1
O10	0.26	0.0	0.517	0.05	1
O11	0.0	0.5	0.0	0.05	1
O12	0.5	0.5	0.0	0.05	1
O13	0.792	0.5	0.948	0.05	1
O14	0.29	0.5	0.949	0.05	1
O15	0.583	0.5	0.898	0.05	1
O16	0.872	0.5	0.847	0.05	1
O17	0.082	0.5	0.897	0.05	1
O18	0.373	0.5	0.847	0.05	1
O19	0.663	0.5	0.796	0.05	1
O20	0.952	0.5	0.745	0.05	1
O21	0.162	0.5	0.796	0.05	1
O22	0.454	0.5	0.745	0.05	1
O23	0.743	0.5	0.694	0.05	1
O24	0.243	0.5	0.694	0.05	1
O25	0.534	0.5	0.643	0.05	1
O26	0.813	0.5	0.578	0.05	1
O27	0.033	0.5	0.644	0.05	1
O28	0.325	0.5	0.593	0.05	1
O29	0.605	0.5	0.525	0.05	1
O30	0.9	0.5	0.474	0.05	1
	R_w	**Scale factor**	**SP diameter**	**d_2**	
	0.58 %	0.82	22 Å	2 Å^2	

Table S5: Refined parameters for the fit seen in Figure 6C in the main text.

	Nb_2WO_8	Space group	Pbcm		
	a	**b**	**c**		
	3.82 Å	18.46	16.02		
	x	**y**	**z**	**U_{iso} (Å^2)**	**occ**
W1	0.949	0.287	0.632	0.006	1
W2	0.978	0.084	0.558	0.006	1
W3	0.081	0.462	0.75	0.006	1
W4	0.077	0.142	0.75	0.006	1
O1	0.467	0.295	0.64126	0.013	1
O2	0.523	0.070	0.545	0.013	1
O3	0.619	0.460	0.75	0.013	1
O4	0.495	0.142	0.75	0.013	1
O5	0.090	0.371	0.538	0.013	1
O6	0.062	0.161	0.646	0.013	1
O7	0.111	0.383	0.680	0.013	1
O8	0.152	0.077	0.672	0.013	1
O9	0.067	0.248	0.75	0.013	1
O10	0.0	0.5	0.5	0.013	1
	R_w	**Scale factor**	**SP diameter**	**δ_2**	
	0.26 %	0.929	23.5 Å	3.11 Å^2	

Table S6: Refined parameters for the fit seen in Figure 7D in the main text.

	Nb_2WO_8	Space group	Pbcm		
	a	**b**	**c**		
	3.83 Å	18.07 Å	15.64		
	x	**y**	**z**	**U_{iso} (Å^2)**	**occ**
W1	0.933	0.220	0.120	0.003	1
W2	0.982	0.420	0.045	0.003	1
W3	0.057	0.046	0.25	0.003	1
W4	0.043	0.364	0.25	0.003	1
O1	0.486	0.202	0.128	0.05	1
O2	0.526	0.406	0.060	0.05	1
O3	0.547	0.024	0.25	0.05	1
O4	0.535	0.343	0.25	0.05	1
O5	0.998	0.166	0.022	0.05	1
O6	0.013	0.309	0.133	0.05	1
O7	0.02	0.093	0.164	0.05	1
O8	0.012	0.439	0.175	0.05	1
O9	0.012	0.224	0.25	0.05	1
O10	0.0	0.0	0.0	0.05	1
	R_w	**Scale factor**	**SP diameter**	**d_2**	
	0.31 %	0.335	17.0 Å	0.99 Å^2	

Table S7: Refined parameters for the fit seen in Figure S28.

	Nb_2WO_8	Space group	Pbcm		
	a	**b**	**c**		
	3.79 Å	18.45 Å	16.07		
	x	**y**	**z**	**U_{iso} (Å^2)**	**occ**
W1	0.962	0.213	0.132343	0.003	1
W2	0.985	0.416	0.057919	0.003	1
W3	0.085	0.037	0.25	0.003	1
W4	0.062	0.358	0.25	0.003	1
O1	0.486	0.202	0.128	0.05	1
O2	0.526	0.406	0.060	0.05	1
O3	0.547	0.024	0.25	0.05	1
O4	0.535	0.343	0.25	0.05	1
O5	0.998	0.166	0.022	0.05	1
O6	0.013	0.309	0.133	0.05	1
O7	0.020	0.093	0.164	0.05	1
O8	0.012	0.430	0.175	0.05	1
O9	0.012	0.224	0.25	0.05	1
O10	0.0	0.0	0.0	0.05	1
	R_w	**Scale factor**	**SP diameter**	**δ_2**	
	0.27 %	0.310	21.0 Å	0.99 Å^2	

Table S8: Refined parameters for the fit seen in Figure 8C in the main text.

	Nb_2WO_8	Space group	Pbcm		
	a	**b**	**c**		
	3.82 Å	18.01 Å	15.62		
	x	**y**	**z**	**U_{iso} (Å^2)**	**occ**
W1	0.934	0.221	0.121	0.004	1
W2	0.986	0.420	0.046	0.004	1
W3	0.073	0.045	0.25	0.004	1
W4	0.061	0.364	0.25	0.004	1
O1	0.483	0.203	0.125	0.01	1
O2	0.523	0.409	0.057	0.01	1
O3	0.546	0.022	0.25	0.01	1
O4	0.540	0.346	0.25	0.01	1
O5	0.0	0.163	0.025	0.01	1
O6	0.017	0.312	0.130	0.01	1
O7	0.024	0.090	0.167	0.01	1
O8	0.009	0.442	0.177	0.01	1
O9	0.010	0.227	0.25	0.01	1
O10	0.0	0.0	0.0	0.01	1
	R_w	**Scale factor**	**SP diameter**	**d_2**	
	0.27 %	0.328	21.0 Å	0.99 Å^2	

E: Total scattering data

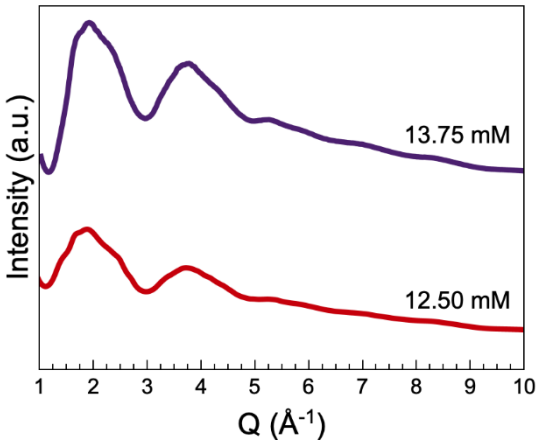

Figure S29: The total scattering data measured from the samples synthesized at 12.50 and 13.75 mM at 250 ºC for 2 h.

References:

1. Mourdikoudis, S.; Liz-Marzán, L. M., Oleylamine in Nanoparticle Synthesis. *Chem. Mater.* **2013,** *25* (9), 1465-1476.
2. Juhas, P.; Farrow, C. L.; Yang, X.; Knox, K. R.; Billinge, S. J. L., Complex modeling: a strategy and software program for combining multiple information sources to solve ill posed structure and nanostructure inverse problems. *Acta Crystallogr. A* **2015,** *71* (6), 562-568.
3. https://www.sasview.org/.
4. Kotlarchyk, M.; Chen, S. H., Analysis of small angle neutron scattering spectra from polydisperse interacting colloids. *J. Chem. Phys.* **1983,** *79* (5), 2461-2469.
5. Percus, J. K.; Yevick, G. J., Analysis of Classical Statistical Mechanics by Means of Collective Coordinates. *Phys. Rev.* **1958,** *110* (1), 1-13.
6. Larsen, A. H.; Pedersen, J. S.; Arleth, L., Assessment of structure factors for analysis of small-angle scattering data from desired or undesired aggregates. *J. Appl. Crystallogr.* **2020,** *53* (4), 991-1005.
7. Li, T.; Senesi, A. J.; Lee, B., Small Angle X-ray Scattering for Nanoparticle Research. *Chem. Rev.* **2016,** *116* (18), 11128-11180.
8. Niu, J.; Zhao, J.; Wang, J.; Bo, Y., Syntheses, spectroscopic characterization, thermal behavior, electrochemistry and crystal structures of two novel pyridine metatungstates. *J. Coord. Chem.* **2004,** *57* (11), 935-946.
9. Averbuch-Pouchot, M. T.; Tordjman, I.; Durif, A.; Guitel, J. C., Structure d'un paratungstate d'ammonium (NH4)6H6W12O42.10H2O. *Acta Crystallogr. B* **1979,** *35* (7), 1675-1677.
10. Momma, K.; Izumi, F., VESTA 3 for three-dimensional visualization of crystal, volumetric and morphology data. *J. Appl. Crystallogr.* **2011,** *44* (6), 1272-1276.
11. Farrow, C. L.; Juhas, P.; Liu, J. W.; Bryndin, D.; Božin, E. S.; Bloch, J.; Th, P.; Billinge, S. J. L., PDFfit2 and PDFgui: computer programs for studying nanostructure in crystals. *J. Phys.: Condens. Matter* **2007,** *19* (33), 335219.
12. Grazulis, S.; Chateigner, D.; Downs, R. T.; Yokochi, A. F. T.; Quiros, M.; Lutterotti, L.; Manakova, E.; Butkus, J.; Moeck, P.; Le Bail, A., Crystallography Open Database - an open-access collection of crystal structures. *J. Appl. Crystallogr.* **2009,** *42* (4), 726-729.

13. Vaitkus, A.; Merkys, A.; Grazulis, S., Validation of the Crystallography Open Database using the Crystallographic Information Framework. *J. Appl. Crystallogr.* **2021,** *54* (2), 661-672.
14. Gražulis, S.; Daškevič, A.; Merkys, A.; Chateigner, D.; Lutterotti, L.; Quirós, M.; Serebryanaya, N. R.; Moeck, P.; Downs, R. T.; Le Bail, A., Crystallography Open Database (COD): an open-access collection of crystal structures and platform for world-wide collaboration. *Nucleic Acids Res.* **2012,** *40* (D1), D420-D427.